SIMULTANEOUS INVERSION OF RECEIVER FUNCTIONS, MULTI-MODE DISPERSION, AND TRAVEL-TIME TOMOGRAPHY FOR LITHOSPHERIC STRUCTURE BENEATH THE MIDDLE EAST AND NORTH AFRICA

Charles J. Ammon[1], Minoo Kosarian[1], Robert B. Herrmann[2], Michael E. Pasyanos[3], William R. Walter[3], and Hrvoje Tkalcic[3]

Penn State University[1], Saint Louis University[2], Lawrence Livermore National Laboratory[3]

Sponsored by Air Force Research Laboratory
and
National Nuclear Security Administration
Office of Nonproliferation Research and Engineering
Office of Defense Nuclear Nonproliferation

Contract No. DE-FC03-02SF22498[1], DTRA01-02-C-0038[2], W-7405-ENG-48[3]

ABSTRACT

This paper reports on the initial investigations into the seismic structure of the lithosphere in the Middle East and North Africa (MENA) using surface waves and receiver functions. Collections of prior work in the region and computing receiver functions, for use in the joint inversion, has been initiated. Critical to the joint inversion is surface-wave dispersion information localized to approximately the same region sampled by receiver functions. We continue to improve our surface-wave dispersion model of western Eurasia and North Africa and have developed group velocity maps at two-degree resolution for both Love and Rayleigh waves from 10 to 100 seconds period. The model shows an excellent relationship to tectonic structure and group velocity variations correlate well with orogenic zones, cratons, sedimentary basins, and rift zones. We have recently implemented a variable-resolution tomography and have pushed the resolution of the model down to one-degree in areas with sufficient density sampling. Our paper presents information on the complexity of the receiver structure at many permanent sites in the region and several illustrative inversions for the lithospheric structure. We have examined receiver functions at over 70 stations in western Eurasia and North Africa and have inverted a number using dispersion measurement from global and regional tomographic models. A comparison of the crustal thickness and Poisson's ratio estimates for the crust beneath these stations will be presented. Other work on the combination of additional observations (body-wave travel times, higher-mode observations, surface-wave polarization information) is planned for future stages of the project, however we include illustrations outlining our ideas for the use of these data to help further constrain the seismic structure of the lithosphere. Access information to on-line information (results, earth models, etc.) will also be provided.

OBJECTIVES

Our objectives are the construction of shear-velocity profiles for regions surrounding broad-band seismic stations throughout the Middle East, central and north Africa, and parts of western Europe. Application of the technique in the MENA region provides an opportunity to revise models of the crust and upper mantle structure throughout the region and to exploit the global and regional work of previous seismic verification research (e.g. Pasyanos *et al.*, 2001; Ritzwoller & Levshin, 1998, Larson *et al.*, 2001). The resulting shear-velocity models provide a single structure consistent with a range of observations and that can be tested as a tool for the construction of mode isolation filters that can help improve the surface-wave magnitude estimate. We also plan to explore the possibility of adding additional data to our inversions of receiver functions and surface-wave dispersion. The diverse seismic activity throughout the region will facilitate cross-validation of the mode isolation filters with simple empirical filters constructed using larger events with adequate signal-to-noise ratios (SNR).

Background

Much of the background for this project is identical to that found in "Simultaneous Inversion of Receiver Functions, Multi-Mode Dispersion, and Travel-Time Tomography for Lithospheric Structure Beneath the Middle East and North Africa", by Ammon *et al.*, which appears elsewhere in these proceedings. We refer the reader to this other work for additional background information.

RESEARCH ACCOMPLISHED

Receiver Function Computation

The first step in this project is the selection of target stations and the computation of receiver functions at those stations. To begin, we have a selected a subset of permanent stations that have relatively long recording histories and thus will have substantial data already available. More recently installed stations and temporary operating stations will be added later in the project. The data processed at the time this report was written are shown in Figure 1. We plan to include all available temporary and permanent stations within central and northern Africa, the Middle East, and parts of Europe. Sixty-nine stations, to date, have been investigated; 36 in Africa, 34 in the Middle East, and 24 stations in southern Europe.

Poisson's Ratio and Crustal Thickness Estimation

As a first step in the receiver function analysis the receiver function stacking method of Zhu and Kanamori [2000] is used to estimate the crustal thickness and Vp/Vs velocity ratio (or Poisson's ratio). The stacking method makes a rather limiting assumption of a uniform crust but the analysis provides good estimates of these quantities when the structure is relatively simple. The estimated values of Poisson's ratios can be used in subsequent inversions that require some assumed value of bulk crustal Poisson's ratio. The current results are summarized in Figure 2. If a station appears twice, that indicates that a significant azimuthal variation was observed (which may indicate a likely failure of this simple imaging approach). Crustal thickness estimates agree on average with the global crustal model 2.0, but at times the differences are significant (greater than 5 km). The mean difference between our results and Crust 2.0 is about 1 km and the standard deviation of the differences is about 7 km, which is larger than the resolution we have on stations with stable receiver functions (probably between, 2.5 to 5 km). The numbers agree more closely when we rank our estimates using the complexity of the observed receiver functions. The estimated Vp/Vs values for each station are shown at the bottom of Figure 2. The shaded region shows a liberal range that is typical for the continental crust. For the most part, our results are showing up lower than average (Zandt and Ammon, 1995). More analysis and the incorporation of quality factors is needed to assess the significance of this observation.

Tomographic Imaging of Group-Velocity Variations

A large-scale study of surface-wave group velocity dispersion across western Eurasia and north Africa (Pasyanos, 2002) has been carried out. This study expands the coverage area northwards relative to previous work (Pasyanos *et al.*, 2001), which covered only north Africa and the Middle East. As a result, we have increased, by about 50%, the

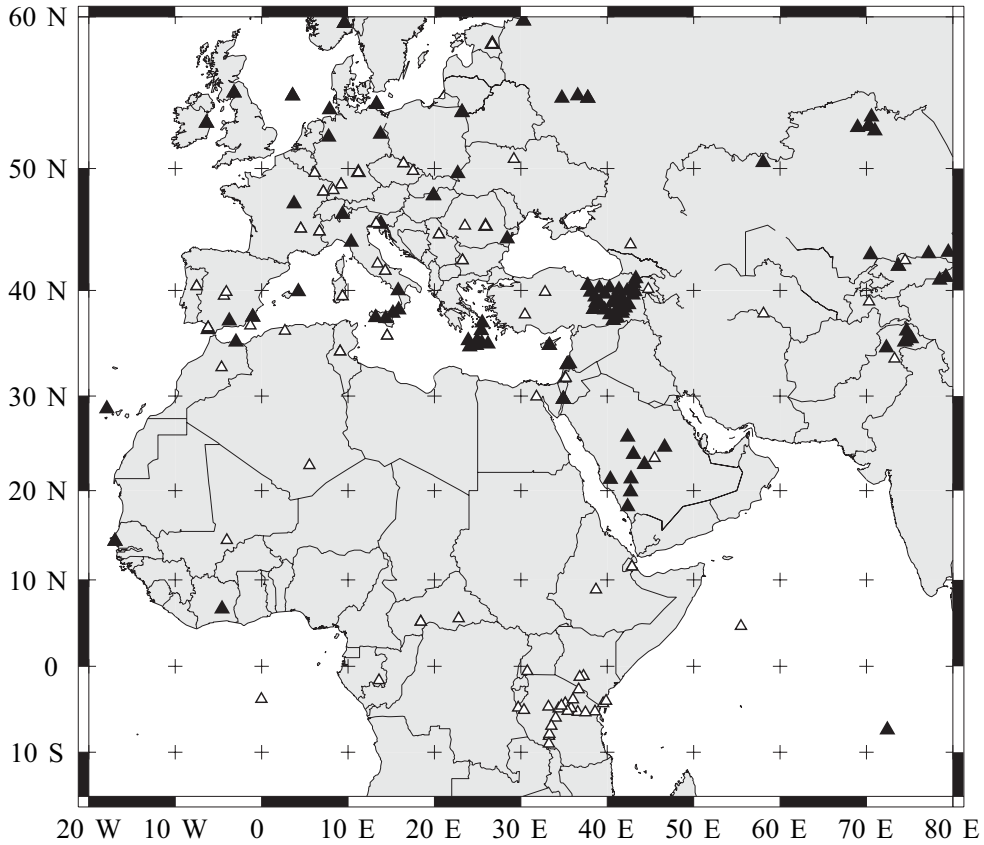

Figure 1. Available permanent and temporary three-component seismic stations in the research area. Shear-wave velocity inversions have been computed for the stations with white triangles. Shaded symbol indicate stations for which we have data, but have not yet completed our analyses.

number of seismograms examined and group velocity measurements made. Good quality dispersion measurements for about 10,000 Rayleigh wave and 6,000 Love wave paths have been made into this study, incorporating measurements from several other researchers. A conjugate gradient method to perform a group velocity tomography was used. We have improved our inversion from the previous study by adopting a variable smoothness (Pasyanos, 2002). This technique allows us to go to higher resolutions, where the data allow, without producing artifacts. Our current results include both Love and Rayleigh wave inversions across the region for periods from 10 to 100 seconds. Figure 3 shows the inversion results for Rayleigh waves at periods of 20 and 50 seconds. Short period group velocities are sensitive to slow velocities associated with large sedimentary features such as the Russian Platform, Mediterranean Sea, and the Persian Gulf. Intermediate periods are sensitive to differences in crustal thickness, such as those between oceanic and continental crust or along orogenic zones. At longer periods, we find fast velocities beneath cratons and slow upper mantle velocities along rift systems and the Tethys Belt.

The Joint Inversion of Receiver Functions and Surface-Wave Dispersion Curves

The receiver function is sensitive to velocity transitions and vertical travel times, surface-wave dispersion measurements are sensitive to aver-ages of the velocities, and relatively insensitive to sharp velocity contrasts. The complementary nature of the signals makes them ideal selections for joint study because they can fill in resolution gaps of each data set. Ammon and Zandt (1993) pointed this out in a study of the Landers region of southern California (although for their specific case, available observations were unsuitable to resolve subtle features in the lower crust) and Özalaybey et al. (1997) and Last et al. (1997) have performed complementary analyses of surface-wave disper-

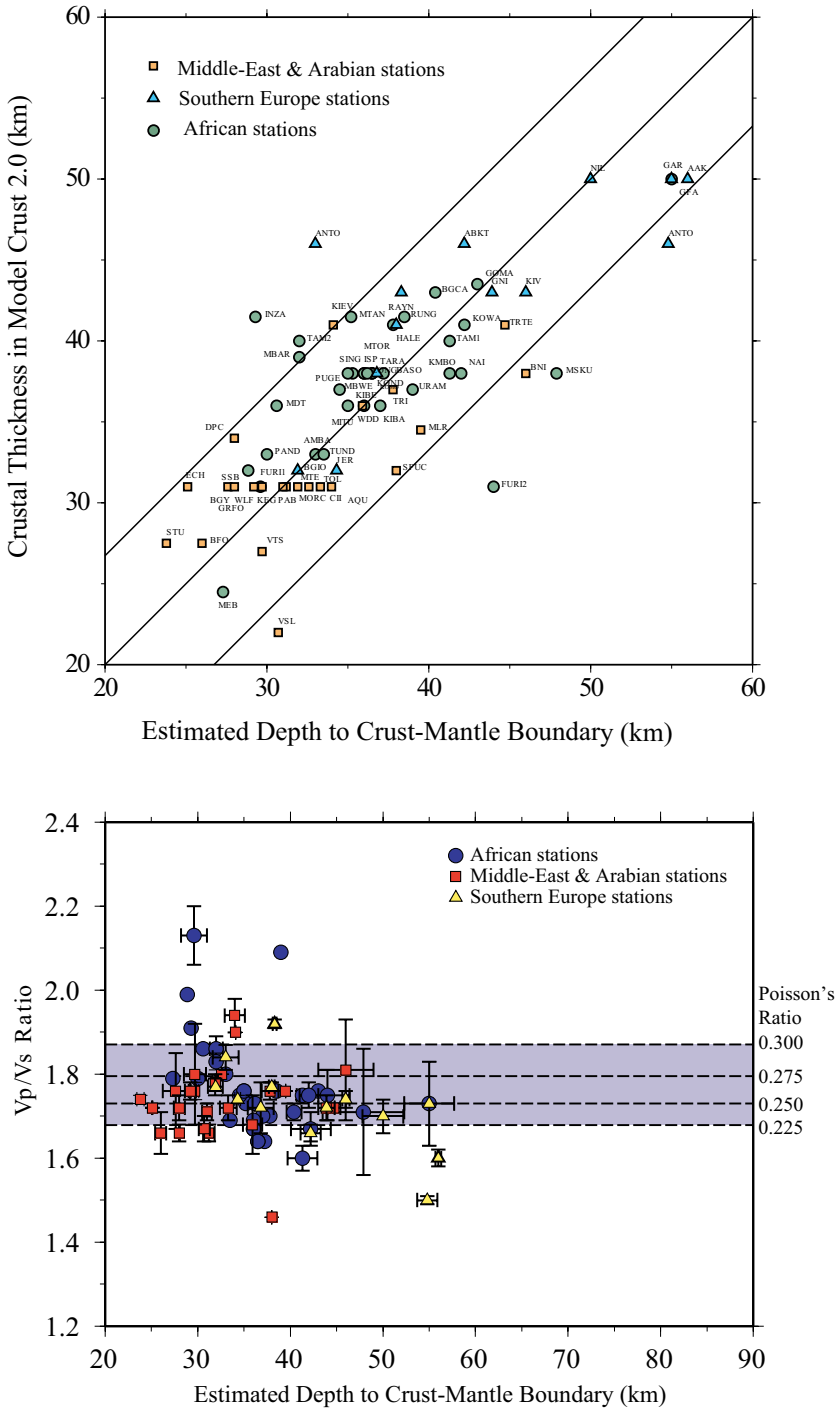

Figure 2. (Top) Comparison of crustal thickness estimated with receiver functions versus values from crustal model 2.0. Stations located in Africa in agreement more with crust 2.0, rather than stations located in Europe and Middle East. It maybe because of heterogeneity and more complicated structure in those regions. (Bottom) Variation of Vp/Vs ratio with crustal thickness, overall trend suggests a decrease in Poisson's ratio with increasing crustal thickness. The depth scale is extended to allow comparison with our results in Asia [Ammon et al., this volume].

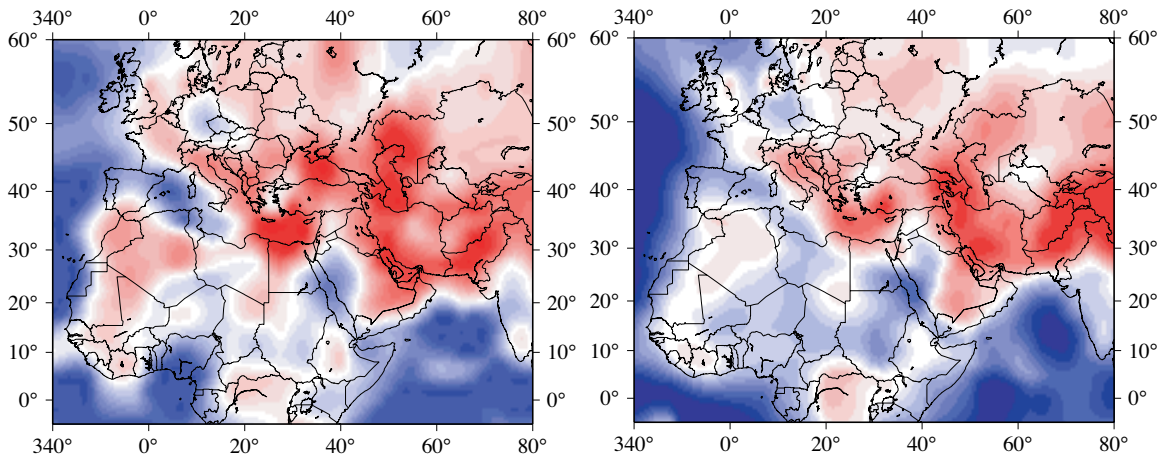

Figure 3. Tomographic imaging results for the Middle East, north Africa, and western Europe. The left diagram shows the lateral group velocity variations in 35-second period Love waves, the map on the right shows the corresponding variations in 35-second period Rayleigh waves. Color scales are relative, blue is fast, red is slow.

sion and receiver functions and Du and Foulger (1999) and Julia *et al*. (2000) implemented joint inversions of these data types. The mechanics of the inversion are relatively simple since partial derivatives of dispersion observations (Herrmann, 1995) and receiver functions waveforms (e.g., Randall, 1989, Ammon *et. al*, 1990) can be calculated quickly and accurately. For more details on the method, we refer the reader to Ammon *et al.* (located elsewhere in these proceedings).

An Example Combined Inversion, Station PUGE, Tanzania

We illustrate the ideas with an example. The results of the inversion of PUGE receiver functions with the Rayleigh-wave group-velocity dispersion values from Pasyanos and Walter [2002] combined with phase velocities digitized from Weeraratne et al [2003] are shown in Figure 4. The fit to the Pasyanos and Walter [2002] dispersion curve is very good and the general fit to the phase-velocities is good. The phase velocities are slightly under-predicted for the shorter periods and over-predicted for the longest periods. The long-period over-prediction is a result of our constraints that the deepest part of the model match that of PREM. Relaxing that assumption would allow the low velocities to extend deeper that 220 km and reduce the deepest average shear-velocity to match the phase velocity. The difference at the shorter periods represents a fundamental difference between the group and phase-velocities. One explanation may be the smoothing of the group velocities has resulted in an artificially lower estimate - very slightly inconsistent with the phase velocities. The receiver functions are very well modeled and produce the relatively smooth crust-mantle transition and crustal thickness (provided with the absolute velocity information from the surface-wave information).The model has a relatively simple crust, consistent with earlier results, and the crust-mantle transition about 7.5 km thick (this could be an intermediate layer at the base of the crust). The mantle structure includes a lid with a thickness of approximately 100 km underlain by a region of low velocities. These velocities are low compared with other shields - consistent with the results of Weeraratne *et al.* [2003]. Although the lid is fast at shallow depths, consistent with regional propagation [e.g. Nyblade and Brazier, 2002; Langston *et al.*, 2002] the model lid is also thinner than usual for an Archean shield.

An Example Combined Inversion, Station KOWA, Mali

In Figure 5 we present the results of the inversion of KOWA receiver functions with the Rayleigh- and Love-wave group-velocity values from Pasyanos and Walter [2002]. The fit to the Pasyanos and Walter [2002] dispersion curve is reasonable, but the complexity in the tomographic dispersion curves is difficult to fit with a lateral homogeneous isotropic earth model. The Love and Rayleigh values appear to be incompatible at the shortest and longest periods (where the tomography has the largest uncertainties).

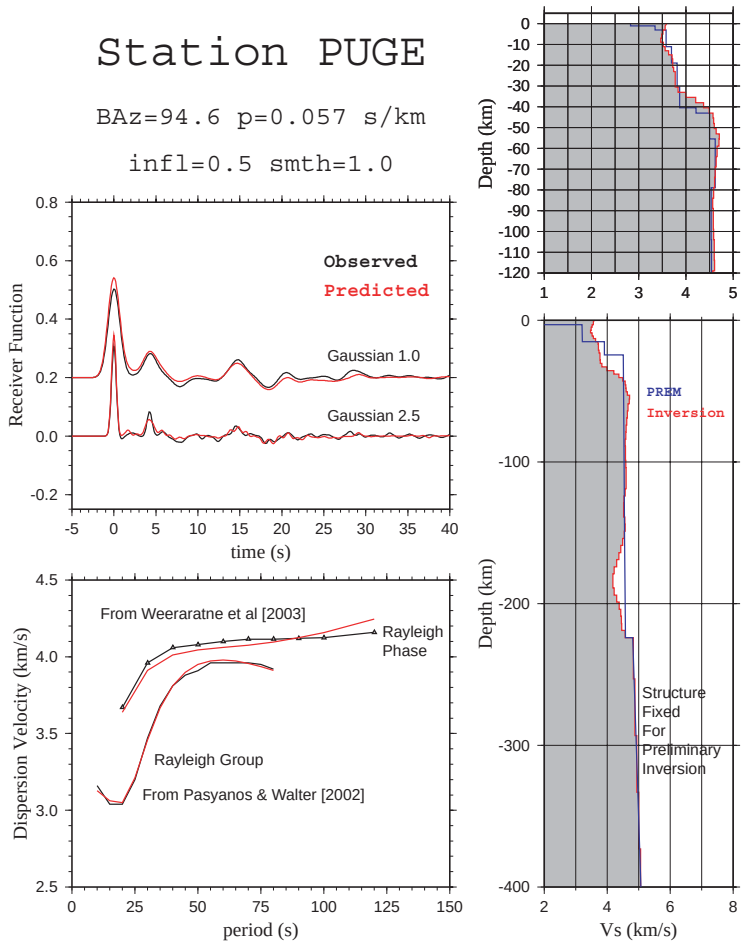

Figure 4. Inversion results for station PUGE using dispersion curves from Pasyanos and Walter [2002] & Weereratne *et al.*, [2003]. The back-azimuth and ray parameter of the incoming P-wave are shown at the top. The influence parameter was 0.5, which balances the weight between the receiver functions and dispersion values, and the smoothness weight was 1.0. The observed and predicted receiver functions in two bandwidths are shown in the upper left, the observed and predicted dispersion curves in the lower left, and the resulting models are shown on the right. The deep structure is constrained to transition smoothly into the PREM - the data have little sensitivity for detailed absolute velocities below approximately 100-150 km. These velocities are earth-flattened by default since we use flat-earth codes to perform the analyses.

The estimated velocity structure has an unusually fast surface layer. This features is to a large part the result of limited resolution in the upper kilometer, and can be removed with increased smoothing near of the shallowest layers with little penalty in the fit to the observations. The mantle lid is faster than PREM, with P-velocities approaching 8.5 km/s at a depth of about 80 km. The lower crust and uppermost mantle have a strong gradient, which could have a large affect on waves turning in that depth such as *Pn* and *Sn*. The low-velocity zone beneath the lid is intriguing. We can remove the structure by increasing smoothing at that depth; the fit to the surface waves degrades marginally, the fit to the arrival at about 233 seconds in the receiver function is worse. To evaluate the structure more carefully will require more data from the station. Despite a rather long formal operation time for KOWA, the number of data useful for receiver functions is limited by frequent gaps in data availability.

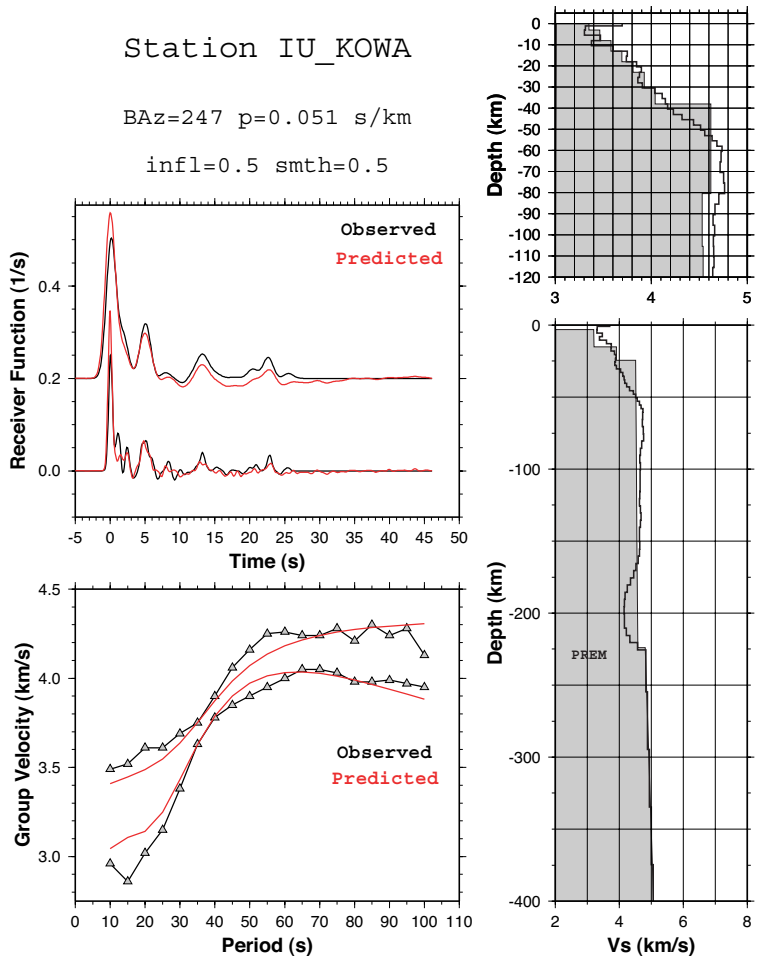

Figure 5. Joint-Inversion result for station KOWA, located in northern Africa. The receiver functions from back-azimuth 247 both in low frequency (0.5 Hz) and high frequency bandwidth of (1.2 Hz) are shown in upper left along with their predictions. Smoothed group velocities from Pasyanos and Walter [2002] with corresponding fit are shown on the lower left. The original and estimated earth models are shown in the upper right. The models have 74 layers with a total thickness of 532 km and the inversion is allowed to vary the upper 225 km. H-K stacking estimated crustal thickness is 42.2±2.15 km with a Vp/Vs = 1.67±0.04. These values calculated from 10 receiver functions, which obtained from 39 available events in the period of 1998-1999 and 2001. For the joint-inversion, smoothness and influence parameters were both 0.5.

An Example Combined Inversion, Station ISP, Isparta, Turkey

Resultsof the inversion of ISP receiver functions with the Rayleigh- and Love-wave group-velocity values from Pasyanos and Walter [2002] are presented in Figure 6 . The observed Love and Rayleigh group velocities are very low, looking almost oceanic at the shorter periods. No short-period Airy phase is evident as the curves plummet to very low velocities at the shortest periods. The fit to the Pasyanos and Walter [2002] dispersion curve is very good. The two receiver functions are the stacks of data from all azimuths and last only about 25 seconds (much of the scattered energy at later times is incoherent and removed by averaging). The early part of the receiver function is complicated in the higher-frequency signal, but relatively simple in the longer period signal. Velocities in the earth model are unusually low, as dictated by the low group velocities. The upper crust is bounded below by a layer with an equivalent P-velocity of about 6.2 km/s. The lower crust begins with a decrease in velocity to an equivalent P-velocity of

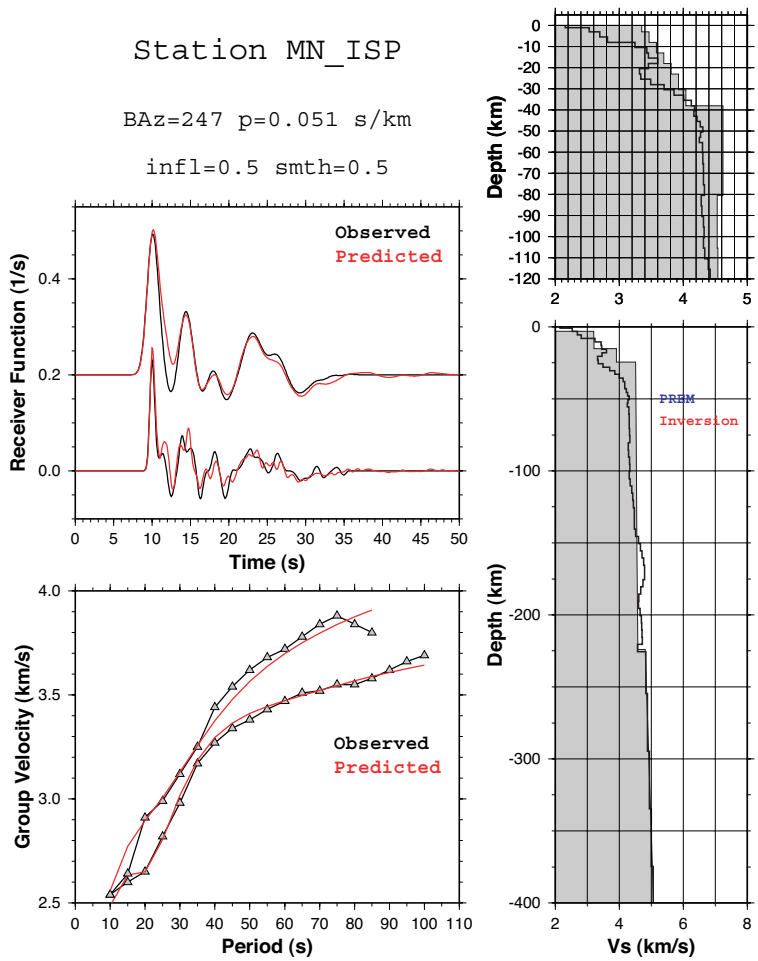

Figure 6. Inversion results for station ISP, located in east-central Turkey. Stacks of 50 receiver functions from all back-azimuth both in low frequency (0.5 Hz) and high frequency bandwidth of (1.2 Hz) are shown in upper left with their predicted ones. Smoothed group velocities from Pasyanos and Walter [2002] with corresponding fit are shown on the lower left. The original and estimated earth models are shown on the right. The model extends to 532 km, but only the upper 225 km are included in the inversion. The H-K stacking crustal thickness estimates is 36.8±1.4 km with a Vp/Vs = 1.72 ± 0.06. These values calculated from 50 receiver functions which obtained from 500 events in the period of 1996-2003.

5.7 km/s, which is underlain by a strong positive velocity gradient. An apparent crust-mantle boundary at a depth of about 30-35 km is very slow - velocities in this depth range are just above 7 km/s. Typical upper mantle velocities of 7.8 and greater are not reached until a depth of 80-90 km.

An Example Combined Inversion, Station HIT, Jordan

In Figure 7 we present the results of the inversion of station HIT receiver functions with the Rayleigh- and Love-wave group-velocity dispersion values from Pasyanos and Walter [2002]. Initial inversions indicated that fitting both Love and Rayleigh dispersion simultaneously was not possible. Separate inversions with the receiver function and Love waves and the receiver function and Rayleigh waves were performed. A similar observation was made for data from station EIL.

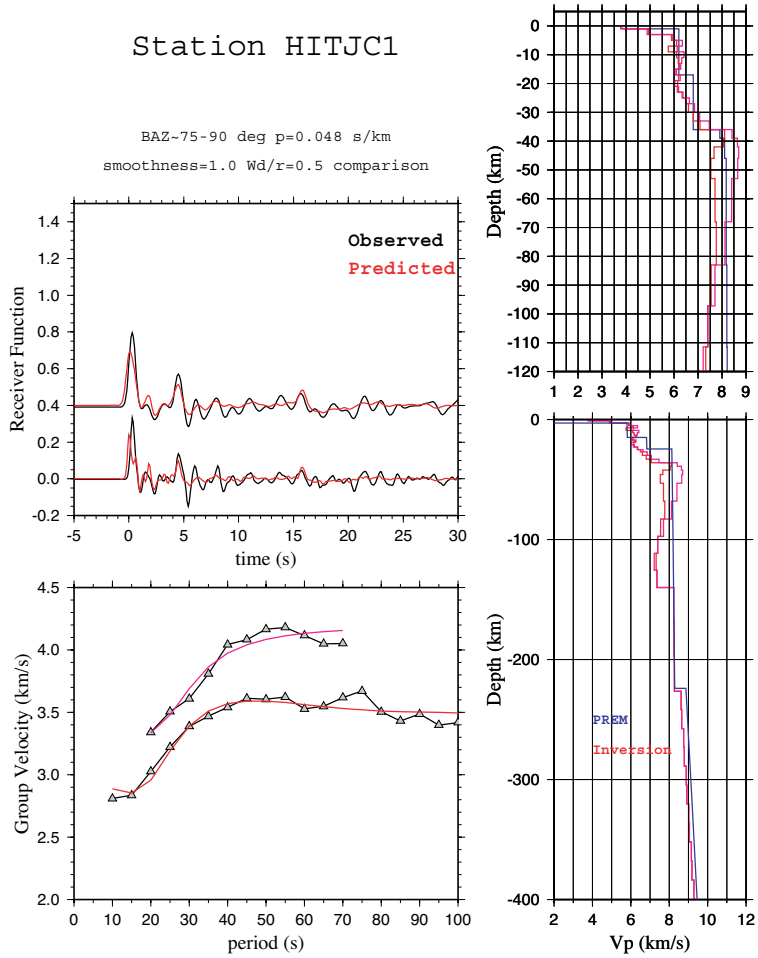

Figure 7. Inversion results for station HIT, Jordan using dispersion curves from Pasyanos and Walter [2002]. Format is similar to earlier presentations except that separate inversions were performed for the Love and Rayleigh wave dispersion curves. The results of the independent inversions are compatible in the crust, but substantially different in the uppermost mantle. Shear velocities have been converted to P-velocities using a standard estimate for Poisson's ratio.

An Example Combined Inversion, Station KBS, Kuwait

The results of the inversion of KBS receiver functions with the Rayleigh- and Love- wave group-velocity dispersion values from Pasyanos and Walter [2002] are presented in Figure 8. The results for three different back-azimuths produce similar fits in all directions. The model in the direction of the Zagros Mountains is approximately 5 km thicker than the results in other directions.

CONCLUSIONS AND RECOMMENDATIONS

Our work is proceeding nicely and most of the permanent stations have been imaged. We are also working with other groups to secure and image structures beneath several more sites in northeastern Africa. We have a few more permanent stations to analyze. We are moving from the initial data collection and preliminary analysis phase into a more expansive interpretation and assessment stage.

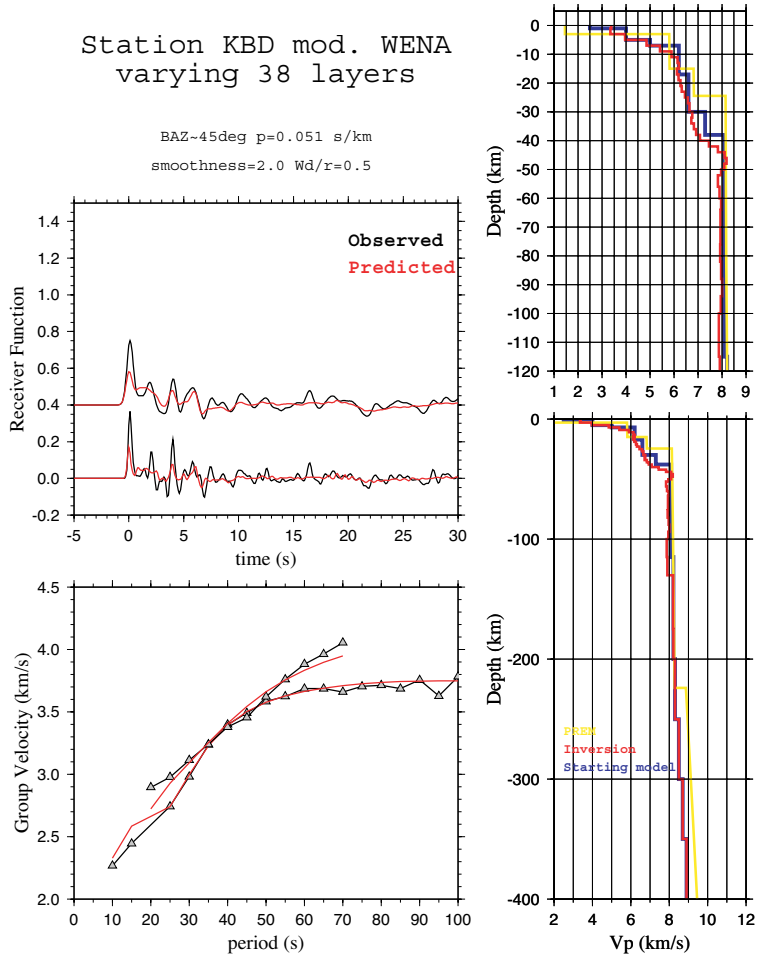

Figure 8. Inversion results for station KBD using dispersion curves from Pasyanos and Walter [2002]. The figure format is similar to earlier examples. Shear velocities have been converted to P-velocities using a standard estimate for Poisson's ratio.

ACKNOWLEDGEMENTS

We thank the P. Wessel and W. H. F. Smith (1990), the authors of GMT for producing easy-to-use, quality software for making maps and charts.

REFERENCES

Ammon, C.J., G.E. Randall, and G. Zandt (1990), On the non-uniqueness of receiver function inversions, *J. Geophys. Res.*, 95, 15303-15318.

Ammon, C.J. (1991), The isolation of receiver effects from teleseismic P waveforms, *Bull. Seism. Soc. Am.*, 81, 2504-2510.

Ammon, C. J., and G. Zandt (1993), The receiver structure beneath the southern Mojave Block, *Bull. Seism. Soc. Am.*, 83, 737-755.

Cassidy, J.F., Numerical experiments in broadband receiver function analysis, *Bull. Seismol. Soc. Am.*, 82, 1453-1474, 1992.

Chevrot, S., and N. Girardin (2000), On the detection and identification of converted and reflected phases from receiver functions, *Geophys. J. Int.*, 141 (3), 801-808.

Clitheroe, G., O. Gudmundsson, and B.L.N. Kennett (2000), Sedimentary and upper crustal structure of Australia from receiver functions, *Australian Journal of Earth Sciences*, 47 (2), 209-216.

Constable, S.C., R.L. Parker, and C.G. Constable (1987), Occam's inversion: A practical algorithm for generating smooth models from electromagnetic sounding data, *Geophysics*, 52, 289-300.

Du, Z.J. and G.R. Foulger (1999), The crustal structure beneath the northwest fjords, Iceland, from receiver functions and surface waves, *Geophys. J. Int.*, 139, 419-432.

Julia, J., C. J. Ammon, R. B. Herrmann, and A. M. Correig (2000), Joint Inversion of receiver function and surface-wave dispersion observations, *Geophys. J. Int.* 143, 99-112.

Kikuchi, M., and H. Kanamori, Inversion of complex body waves (1982), *Bull. Seism. Soc. Am.*, 72, 491-506, 1982.

Langston, C.A. (1979), Structure under Mount Rainier, Washington, inferred from teleseismic body waves, *J. Geophys. Res.*, 84, 4749-4762.

Larson, E. W. F. and G. Ekström (2001), Global Models of Group Velocity, *Pure and Applied Geophys.*, 158, 1377-1399.

Levin, V., and J. Park (1997), Crustal anisotropy in the Ural Mountains from teleseismic receiver functions, *Geophysical Research Letters*, 24 (11), 1283-1286.

Ligorría, J.P. (2000), An Investigation of the Crust-Mantle Transition Beneath North America and the Bulk Composition of the North American Crust, *Ph.D. Thesis, Saint Louis University*, 261 pages.

Ligorría, J.P. and C. J. Ammon (1999), Iterative deconvolution and receiver function estimation, *Bull. Seismol. Soc. Am.*, 89, 1395-1400.

Myers, S.C., and S.L. Beck (1994), Evidence for a local crustal root beneath the Santa Catalina metamorphic core complex, Arizona, *Geology*, 22, 223-226.

Owens, T.J., G. Zandt, and S.R. Taylor (1984), Seismic evidence for an ancient rift beneath the Cumberland Plateau, Tennessee: A detailed analysis of broadband teleseismic P waveforms, *J. Geophys. Res.*, 89, 7783-7795.

Özalaybey, S., M.K. Savage, A.F. Sheehan, J.N. Louie, and J.N. Brune (1997), Shear-wave velocity structure in the northern Basin and Range Province from the combined analysis of receiver functions and surface waves, *Bull. Seismol. Soc. Am.*, 87, 183-199.

Park, J., and V. Levin (2000), Receiver functions from multiple-taper spectral correlation estimates, *Bull. Seismol. Soc. Am.*, 90 (6), 1507-1520.

Pasyanos, M.E., W.R. Walter, and S.E. Hazler (2001), A Surface wave dispersion study of the Middle East and North Africa for Monitoring the Comprehensive Nuclear-Test-Ban Treaty, *Pure and Applied Geophys*, 158, 1445-1474.

Pasyanos, M.E., and W.R. Walter, Crust and upper-mantle structure of North Africa, Europe and the Middle East from inversion of surface waves, Geophys. J. Int., 149, 463-481, 2002.

Pasyanos, M.E. (2002), A Variable-resolution Surface Wave Dispersion Study of Western Eurasia and North Africa, submitted to *Journal of Geophysical Research*.

Ritzwoller, M. H. and A. L. Levshin (1998), Eurasian surface wave tomography: Group velocities, *J. Geophys. Res., 103*, 1839-1878.

Ryberg, T., and M. Weber (2000), Receiver function arrays; a reflection seismic approach, *Geophys. J. Int.*, 141 (1), 1-11.

Sandvol, E., D. Seber, A. Calvert, M. Barazangi (1998), Grid search modeling of receiver functions: Implications for crustal structure in the Middle East and North Africa, *J. Geophys. Res.*,103, 26,899-26,917.

Savage, M.K. (1998), Lower crustal anisotropy or dipping boundaries? Effects on receiver functions and a case study in New Zealand, *J. Geophys. Res.*, 103 (7), 15,069-15,087, 1998.

Stevens, J. L. and K. L. McLaughlin (2001), Optimization of Surface Wave Identification and Measurement, *Pure and Applied Geophys*., 158, 1547-1582

Su, W., R. L. Woodward, and A. M. Dziewonski (1994), Degree 12 model of shear velocity heterogeneity in the mantle, *Nature*, 99, 6945-6980.

Weeraratne, D.S., D.W. Forsyth, K.M. Fischer, and A.A. Nyblade, Evidence for an upper mantle plume beneath the Tanzanian craton from Rayleigh wave tomography, J. Geophys. Res., 2002JB002273R, 2003.

Zandt, G., and C. J. Ammon (1995), Continental Crustal composition constrained by measurements of crustal Poisson's ratio, *Nature*, 374, 152-154.

Zandt, G., S.C. Myers, and T.C. Wallace (1995), Crust and mantle structure across the Basin and Range-Colorado Plateau boundary at 37 degrees N latitude and implications for Cenozoic extensional mechanism, *J. Geophys. Res.*, 100 (6), 10,529-10,548.

Zhu, L., and H. Kanamori (2000), Moho depth variation in Southern California from teleseismic receiver functions, *J. Geophys. Res.*, 105 (2), 2969-2980.